The conformation of the Congo-red ligand bound to amyloid fibrils HET-s(218–289): a solid-state NMR study

The conformation of the Congo-red ligand bound to amyloid fibrils HET-s(218-289): A solid-state NMR study

Chandrakala Gowda,[1] Giorgia Zandomeneghi,[1] Herbert Zimmermann,[2] Anne K. Schütz,[1] Anja Böckmann,[3] Matthias Ernst,[1]* and Beat H. Meier[1]*

* Corresponding authors

[1] Physical Chemistry, ETH Zurich, 8093 Zurich, Switzerland

E-mail: beme@ethz.ch, maer@ethz.ch

[2] Department of Biomolecular Mechanisms, Max-Planck-Institut für medizinische Forschung, Jahnstr. 29, 69120 Heidelberg, Germany

[3] IBCP, UMR 5086 CNRS/Université de Lyon 1, 7 Passage du Vercors, 69367 Lyon, France

ORCID Numbers:

Giorgia Zandomeneghi: 0000-0001-9452-8751
Herbert Zimmermann: 0000-0002-1653-6702
Anne K. Schütz: 0000-0001-6398-5757
Anja Böckmann: 0000-0001-8149-7941
Matthias Ernst: 0000-0002-9538-6086
Beat H. Meier: 0000-0002-9107-4464

Keywords

MAS, Amyloid fibrils, Congo red, rotor-synchronized tensor-correlation experiments

Acknowledgements

We would like to thank Albert A. Smith for helpful discussions. This work has been supported by the Swiss National Science Foundation SNF (grant 200020_159707 and 200020_146757) and by the French ANR (ANR-14-CE09-0024B)

Abstract

We have previously shown that Congo red (CR) binds site specifically to amyloid fibrils formed by HET-s(218-289) with the long axis of the CR molecule roughly parallel to the fibril axis. HADDOCK docking studies indicated that CR adopts a roughly planar conformation with the torsion angle ϕ characterizing the relative orientation of the two phenyl rings being a few degrees. In this study, we experimentally determine the torsion angle ϕ at the center of the CR molecule when bound to HET-s(218-289) amyloid fibrils using solid-state NMR tensor-correlation experiments. The method described here relies on the site-specific ^{13}C labeling of CR and on the analysis of the two-dimensional magic-angle spinning tensor-correlation spectrum of $^{13}C_2$-CR. We determined the torsion angle ϕ to be 19±1°.

Introduction

Several neurodegenerative pathologies are characterized by the presence of amyloid deposits composed of β-sheet rich proteins and the dye Congo red (CR) (Fig. 1a) is a gold standard to detect their presence *in vitro* and in histology[1] by observing the characteristic apple-green birefringence pattern under polarized light[2-4]. Congo red also represents an interesting model system to understand the binding mechanisms of dye or marker molecules to amyloid fibrils and the corresponding conformational changes of the dye molecule[5]. The presence of extensive cross β-sheet structures in amyloid fibrils is considered necessary for CR binding and birefringence. This is, however, neither a necessary nor a sufficient condition[6,7]. For example, it has been observed that upon a single point mutation in HET-s(218-289) at Lys229 to alanine, a mutation which preserves the β-sheet rich secondary structure of the protein, CR fails to bind to the corresponding amyloid fibrils[8].

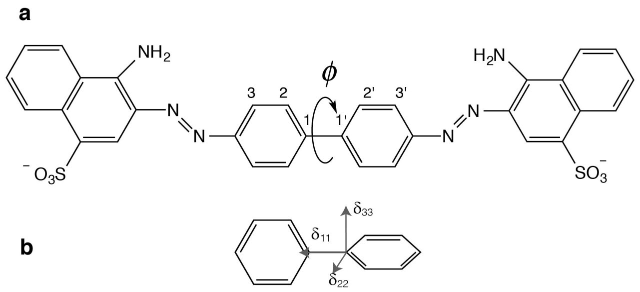

Fig. 1 a Congo red (CR), with the torsion angle ϕ to be investigated. **b** Approximate ^{13}C CSA tensor orientation at C_1' in the molecular frame of the biphenyl ring.

As shown in Fig. 1a, the biphenyl group at the center of CR, enclosed by two diazo groups, each bound to a naphthyl ring, constitutes the hydrophobic portion of the molecule. An amino and a sulfonate group (the latter is negatively charged at neutral pH) bound to each of the naphthyl rings comprise the hydrophilic part.

Solid-state NMR and HADDOCK docking studies have shown that CR binds site-specifically to HET-s(218-289) amyloid fibrils with the long axis of the CR molecule roughly parallel to the fibril axis. The conformation of the protein remains largely undisturbed upon CR bindng[8]. Electrostatic interactions between the two negatively charged sulfonate groups and the NH_3^+ of the Lys229 residues on the *i* and the *i+2* monomer of the fibril are the main interactions that drive and stabilize the CR binding to HET-s(218-289). In addition, the amine groups of CR cab form hydrogen bonds with the residues Ala228 and Ser263.[8]

The positively charged lysine residues that form binding sites on the *i* and *i+2* monomers of the fibril, separated by ~19 Å, matching the separation between the negatively charged sulfonate groups on CR, when in roughly planar conformation. HADDOCK docking leads indeed to a roughly planar conformation with ϕ = 5±3° (see Fig. 1 for the definition of ϕ)[8], also observed by UV Raman spectroscopy.[9] In the solution state, CR was found to be twisted[9,10]. The torsion angle ϕ of CR bound to amyloids has not yet been directly measured.

In this contribution, we use solid-state NMR spectroscopy, in particular two-dimensional (2D) magic-angle spinning (MAS) rotor-synchronized tensor-correlation experiments[11-13], to determine the torsion angle ϕ in CR bound to HET-s(218-289) amyloid fibrils. The application of MAS enhances the signal-to-noise ratio of the experiment and facilitates the quantitative analysis of the data[14].

Materials and Methods

Synthesis of selectively ^{13}C-labeled sodium salt of Congo red

1,1'-$^{13}C_2$-labeled Congo-red with 99% labeling degree was prepared by tetrazotizing 1,1'-$^{13}C_2$-benzidine and coupling with sodium naphthionate. The 1,1'-$^{13}C_2$-labeled benzidine was synthesized out of 1,1'-$^{13}C_2$-labeled 4,4'-dibromobiphenyl by amination with ammonia and cupper salts and bronze as catalysts under pressure. The 1,1'-$^{13}C_2$-labeled 4,4'-dibromobiphenyl was obtained by gas-phase bromination of 1,1'-$^{13}C_2$-biphenyl. The latter was realized by Ullmann homocoupling of 1-^{13}C-bromobenzene with palladium on charcoal as catalyst in ethyleneglycol, and NaOH as base.

In the following, we describe in detail the key steps of the synthesis of 1,1'-$^{13}C_2$-labeled biphenyl and the amination of the 1,1'-$^{13}C_2$-labeled 4,4'-dibromobiphenyl to the benzidine. The bromination of the biphenyl, the tetrazotisation of the benzidine, and the coupling with sodium naphthionate (Aldrich) to Congo red are standard procedures and will not be described here.

1,1'-$^{13}C_2$-labeled biphenyl

Ethyleneglycol (520 mg) and 1-^{13}C bromobenzene (1.3 grams, Deutero GmbH, Kastellaun, Germany) were added to 2.3 ml H_2O and 0.7 grams NaOH–pellets in a 100 ml round-flask with a reflux-condenser together with 500 mg Pd/C 10%. The mixture was stirred and heated under reflux for 20 hours. Some of the obtained biphenyl sublimed into the cooler. After cooling to room temperature, the mixture was extracted with methylenechloride and evaporated. The obtained crystalline solid was purified by column chromatography (Silica, n-hexane), giving 1,1'-$^{13}C_2$-biphenyl with 80% yield.

1,1'-$^{13}C_2$-labeled benzidine

1,1'-$^{13}C_2$-labeled 4.4'-dibromobiphenyl (980 mg) together with 0.72 grams Cu-bronze, 50 mg Cu(I)bromide, 50 mg Cu(II)bromide and 15 ml conc. aqueous ammonia were heated and stirred at 190-205 °C in a closed high-pressure vessel for 24 hours. After cooling the mixture was extracted 3x with ethylacetate, washed with conc. NaCl solution and evaporated to dryness. The product was purified by column chromatography (Silica, mobile phase: ether/ethylacetate 4:1); 335 mg 1,1'-$^{13}C_2$-labeled benzidine was obtained.

From all the intermediates and the final Congo red product we have measured mass-spectra as well as ^{13}C-NMR spectra and we assessed excellent chemical and isotopic purity.

Preparation of [^{2}H, ^{15}N]-labeled HET-s(218-289) fibrils

[^{2}H, ^{15}N]-labeled HET-s(218-289) with a C-terminal His_6 tag was recombinantly expressed in *Escherichia coli* BL21 using deuterated M9 minimal medium, which contained D_2O, perdeuterated glucose as the sole carbon source and $^{15}NH_4Cl$ as the sole nitrogen source. The expression, purification and fibrilization procedure has been described previously[15].

Preparation of $^{13}C_2$-CR bound to HET-s(218-289) fibrils

Approximately 10-fold molar excess of $^{13}C_2$-CR dissolved in D_2O was added to the fibrils left at room temperature for 3 days with gentle shaking at regular intervals. The sample was washed with 25-30 ml of D_2O

and centrifuged subsequently to remove the supernatant, which consisted of unbound Congo red. The washing procedure was repeated 6 times until the supernatant was colorless.

NMR measurements

The spectra of $^{13}C_2$-CR bound to HET-s(218-289) fibrils were recorded on a Bruker Avance-III 850 MHz wide-bore spectrometer (20 T). All experiments were performed using a Bruker 3.2 mm triple-resonance probe.

The 2D MAS tensor-correlation experiments were recorded using the pulse sequence shown in Fig. 3, which has been adapted from reference[12,13]. Two datasets I and II were recorded: in dataset I the time period t_{mix} was rotor synchronized, while in dataset II the time period t_1+t_{mix} was rotor synchronized. States-type data acquisition was employed. Each t_1 point thus resulted in four FIDs. The data were combined as previously described[12,13] using a MATLAB (The MathWorks, Inc., Natick, MA, U.S.A.) script to obtain pure absorptive peaks. A total of 136 t_1 points for dataset I and for dataset II were acquired (thus, 136*4 = 544 FIDs) with 320 scans each using a recycle delay of 2.5 s. The synchronization of the mixing times with sample spinning has been tested on a sample of U-[^{13}C, ^{15}N]-labeled alanine (see Fig. S2, Supplementary Material).

The full experimental parameters are reported in Tables S1 and S2 in the Supplementary Material. All spectra were processed using matNMR[16]. ^{13}C NMR spectra were referenced externally to the methylene signal of adamantane at 38.48 ppm relative to tetramethylsilane (TMS). Sample temperature was about 20 °C.

Spectral analysis

The 1D CPMAS spectrum of $^{13}C_2$-CR bound to HET-s(218-289) (Fig. 2a) was fitted using the peakfit routine in matNMR[16], assuming that the natural abundance aromatic ^{13}C carbons in CR give rise to the lower frequency shoulder (indicated by red lines in Fig. 2a) of the main peak assigned to $^{13}C1/^{13}C1'$. The experimental and fitted spectra, as well as the difference, are shown in Fig. S1 in Supplementary Material.

The Herzfeld and Berger CSA analysis[17] has been performed using the HBA software[18].

The 2D MAS tensor-correlation spectrum of $^{13}C_2$-CR bound to HET-s(218-289) (Fig. 2b) was processed as described[13] (see also Supplementary Material). Nine spinning sidebands associated to $^{13}C_2$-CR were clearly visible along the diagonal of the 2D spectrum and the integrals corresponding to 9 x 9 (potential) cross peaks have been determined using MATLAB. The 2D MAS polarization-transfer spectrum was simulated using the GAMMA spin-simulation environment[19] based on the analytical solutions of CSA tensor correlation spectroscopy under MAS[12,13]. As relative orientation (α, β, γ) of the CSA tensors at C1 and C1' the value α = 90°, γ = 90° and $\beta = \phi$ were used with β ranging from 0° to 90° in steps of 1°. The resulting 2D simulated spectra were analyzed and the intensities corresponding to the 9 x 9 cross peaks were compared to the experimental values.

HADDOCK docking

HADDOCK docking was performed as already described.[8] The experimentally determined torsion angle ϕ = 19° between the biphenyl rings in CR was included as a dihedral angle restraint with an exponent of two and a force constant of 50 (relative to a force constant 1 for unambiguous distance restraints). The addition of the dihedral angle did not lead to an increase in restraint violation energies. The docking parameters obtained with and without the dihedral angle restraint are indeed identical within the error and detailed in Table S3 in Supplementary Material.

Results

CSA tensor determination

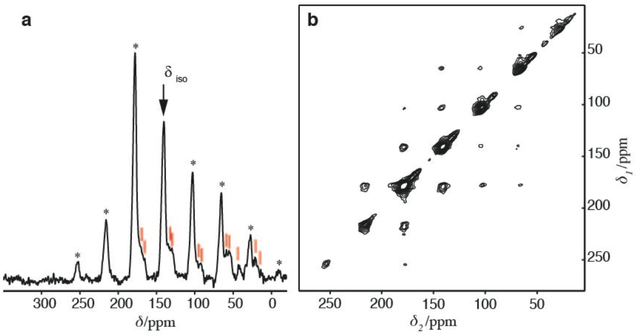

Fig. 2 ^{13}C NMR MAS spectra of $^{13}C_2$-labeled Congo red bound to [^2H, ^{15}N]-labeled HET-s(218-289) fibrils measured at a spinning frequency of 8 kHz and at a static magnetic field of 20 T **a** 1D CPMAS spectrum. δ_{iso} indicates the isotropic chemical shift, while asterisks designate the spinning sidebands of the $^{13}C_2$–CR signal and red lines the signals from natural abundant carbons. **b** 2D MAS tensor-correlation spectrum acquired using rotor-synchronized spin diffusion (50 ms) for the mixing

The carbon spin at C1 and C1' have a sizable chemical-shift anisotropy (CSA) tensor. In crystalline *p*-Xylene, for example, the CSA tensor is oriented as shown in Fig. 1 with the least-shielded principal axis deviating not more than 3° (1°±2°) from the C-C bond[20]. The C1 and C1' spins have identical CSA principle values, but different orientation. The ^{13}C MAS spectrum of $^{13}C1_2$-CR bound to [^2H, ^{15}N]-labeled HET-s(218-289) consists of a main resonance with its sidebands as well as minor contributions from the natural abundance signals from other atoms in the CR and possibly from the protein (Fig. 2(a)).

The principal values of the CSA tensor were determined by fitting the integrated intensities of the spinning-sideband manifold using a Herzfeld and Berger analysis[17]. The effect of the one-bond ^{13}C-^{13}C dipolar coupling on the CSA-tensor determination is minor (see Supplementary Material) and has been neglected in the analysis. The tensor values obtained are δ_{11}=233±3 ppm, δ_{22}=169±2 ppm, δ_{33}=20±2 ppm. The isotropic chemical-shift value of the CR 1-^{13}C is δ_{iso} = 140.5 ppm (all values relative to TMS).

The line widths of the resonances are relatively broad, on the order of 6 ppm (FWHM). The homonuclear dipolar broadening of C1 and C1' ("*n*=0 rotational resonance")[21] accounts for a line width contribution of ~3 ppm, as simulated by Simpson[22]. The additional line width is probably due to a heterogeneous broadening connected to structural inhomogeneity.

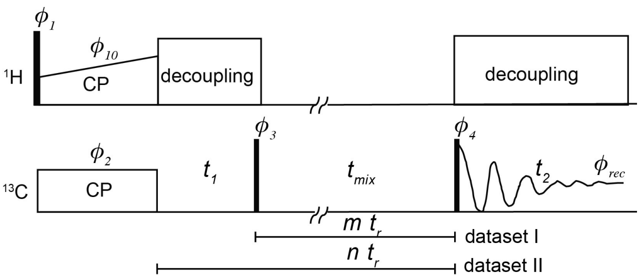

Fig. 3 Pulse sequence for the 2D tensor-correlation experiment, adapted from reference[13]. The time t_1 is the indirect evolution time, t_{mix} is the polarization-transfer time, t_2 the direct evolution time and t_r is the rotor period. *m*, *n* are integers. Phase cycle (in multiples of 90°): ϕ_1=1 3; ϕ_2=0; ϕ_3=1 1 3 3; ϕ_4= 3 3 3 3 0 0 0 0 1 1 1 1 2 2 2 2; ϕ_{10}=0; ϕ_{rec}=0 2 2 0 1 3 3 1 2 0 0 2 3 1 1 3

Tensor-correlation experiments to determine relative CSA tensor orientation

We have measured 2D MAS tensor-correlation experiments using spin-diffusion polarization transfer with rotor-synchronized mixing, as shown in Fig. 3 (see also "Materials and Methods"). Off-diagonal peaks arise from intramolecular $^{13}C1$-$^{13}C1'$ proton-driven spin-diffusion polarization transfer. The intensity pattern of the cross peaks is determined by the relative orientations of the two CSA tensors within the CR molecule[14,23]. The 2D tensor-correlation spectrum of $^{13}C_2$-CR bound to HET-s(218-289) fibrils with a 50 ms spin-diffusion mixing time (see Fig. 2S in Supplementary Material for the determination of the mixing time) is shown in Fig. 2(b). The signals due to natural-abundance carbons from the other carbon sites in CR and possibly the protein appear only as elongations of the diagonal peaks and do not influence the cross peak intensities (see insert in Fig. S3(a), Supplementary Material).

Simulations of the 2D polarization-transfer spectrum

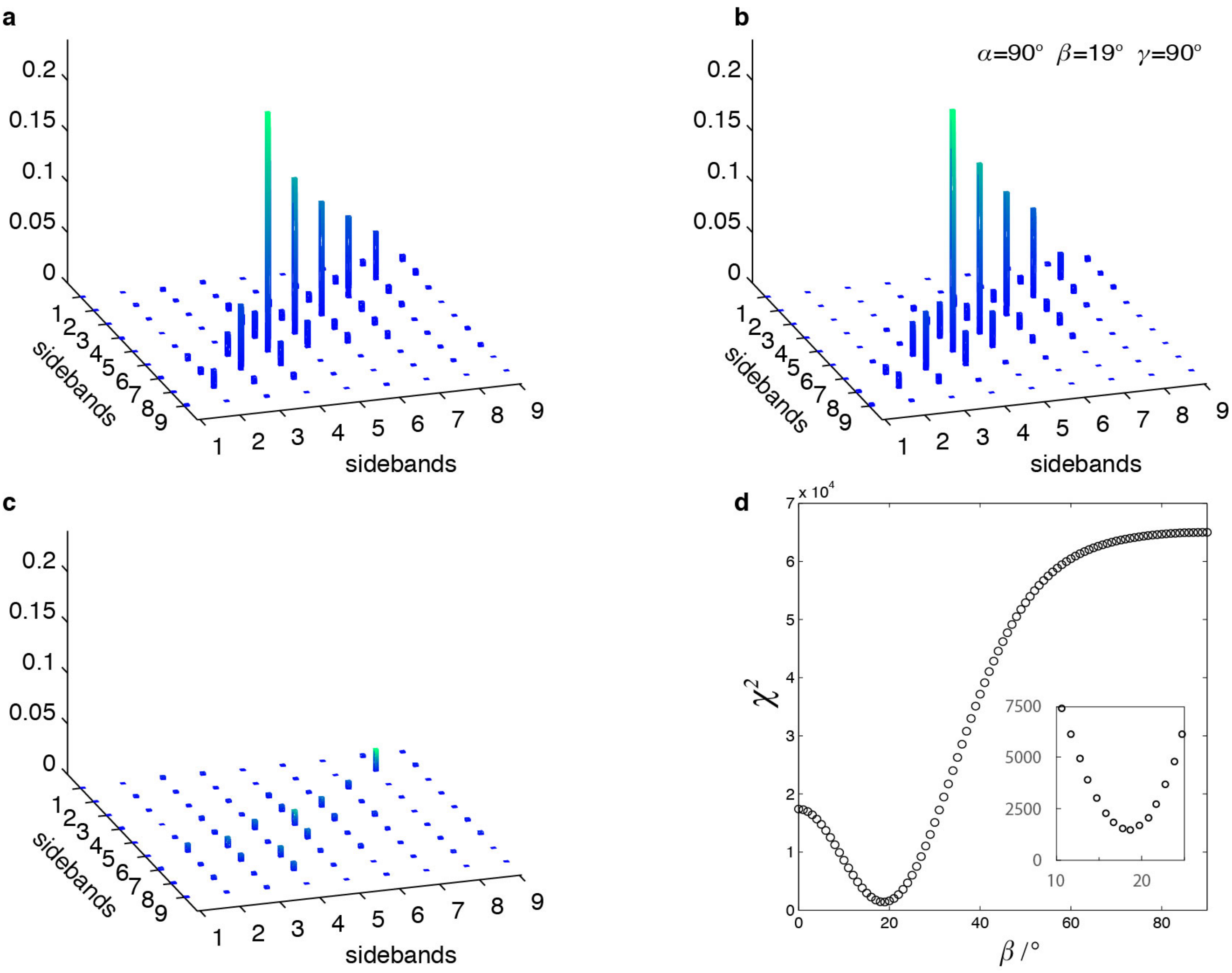

Fig. 4 Bar plot representation of peak integrals: **a** Experiment reported in Fig. 2b. **b** Best matching simulation at β=19° of the experimental data in **a**. **c** Difference between the experiment and the simulated intensities. **d** χ^2 values of the least square fit of the experimental peak integrals with that of the simulated intensities and detail with the distribution of χ^2 values around the minimum

The 2D sideband pattern in the tensor-correlation spectrum defines the relative orientation of the CSA tensors at sites C1 and C1'. To derive the molecular geometry from these data, the orientation of the chemical-shift tensor in the molecular frame must be known. Studies of model systems have shown that the orientation is to a good approximation as shown in Fig. 1b, with the least-shielded axis aligned with the C-C bond, and the other two in the plane of the ring and orthogonal to it[20,24]. In general, the orientation of the CSA tensor at the C1' atom with respect to the CSA tensor at the C1 is defined by three Euler angles (α, β, γ). With the specific CSA tensor orientation in the molecular frame, the relative orientation of the CSA tensors at C1 and C1' simplifies to α = 90° and γ = 90° with $\beta = \phi$. The experimental C1/C1' peak intensities from Fig. 2b) were measured and are represented in the bar plot of Fig. 4(a). Using these data, the angle β that explains the experimental data best was determined using a grid search with 1° resolution. The χ^2 values for the different β values are shown in Fig. 4(d). The minimum value is obtained at a torsion angle β = 19°. The best-fit simulation for the experimental spectrum and the difference with respect to the experimental spectrum are shown in Figs. 4(b) and 4(c), respectively. There is a small systematic deviation, which indicates that the diagonal peaks are too high in the fit and the cross peaks too weak. This can be explained by incomplete polarization transfer, by the presence of singly ^{13}C1 labeled CR molecules or by some background signal which does not contribute to the exchange process.

The statistical error is estimated using Monte Carlo methods: White Gaussian noise is added to the simulated spectra and the least square fitting with the experimental spectra is performed to obtain the torsion angle. The process is repeated several times, each trial of fitting using different white Gaussian noise. The statistical error was found to be 1° (see Supplementary Material for details).

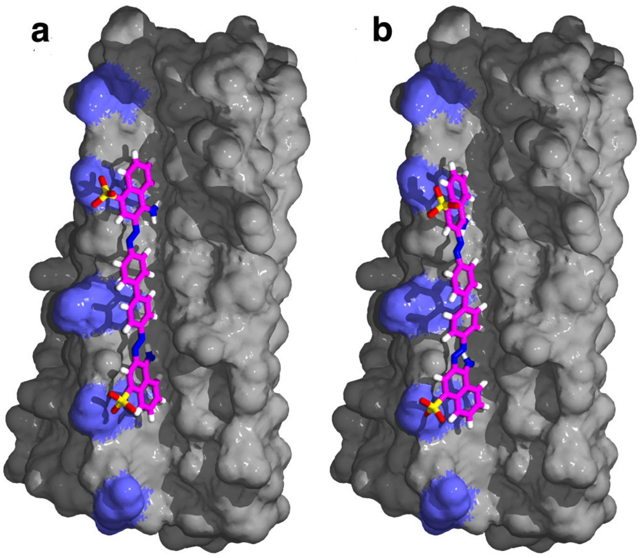

Fig. 5 Side-view of the complex with CR shown in stick representation with CPK colouring docked to the HET-s(218–289) fibril in surface representation with residue K229 marked in purple. A: The CR conformation in the unrestrained case. B: The CR conformation when restrained to $\phi = 19^\circ$

HADDOCK docking

When including the experimentally determined torsion angle $\phi = 19^\circ$ as a restraint into the HADDOCK docking calculation, docked complexes (Fig. 5) and docking parameters (Table S3) very similar to the unrestrained case[8] are obtained. Thus, the experimental value $\phi = 19^\circ$ is compatible with the binding mode found earlier[8] and further refines the docked complex.

Conclusions

We experimentally determined the torsion angle of the biphenyl bond at the center of the Congo red molecule when bound to HET-s(218-289) amyloid fibrils. The method used relies on the specific double ^{13}C labeling of the CR molecule and on the analysis of the 2D MAS tensor-correlation spectrum of $^{13}C_2$-CR bound to HET-s(218-289). We determined the torsion angle ϕ to be $19\pm1^\circ$. This value corresponds to the relative orientation of the principal axes of the two CSA tensors. For the relative orientation of the ring-fixed molecular coordinate systems an additional systematic error of a maximum of 3° per tensor should be considered.

References

1. Westermark, P. *et al.* A primer of amyloid nomenclature. *Amyloid* **14,** 179–183 (2007).
2. Puchtler, H., Sweat, F. & Levine, M. On Binding of Congo Red by Amyloid. *J. Histochem. Cytochem.* **10,** 355–364 (1962).
3. Benditt, E. P., Eriksen, N. & Berglund, C. Congo red dichroism with dispersed amyloid fibrils, an extrinsic cotton effect. *Proc. Natl. Acad. Sci. USA* **66,** 1044–1051 (1970).
4. Frid, P., Anisimov, S. V. & Popovic, N. Congo red and protein aggregation in neurodegenerative diseases. *Brain Res. Rev.* **53,** 135–160 (2007).
5. Herrmann, U. S. *et al.* Structure-based drug design identifies polythiophenes as antiprion compounds. *Sci. Transl. Med.* **7,** –299ra123 (2015).
6. Khurana, R., Uversky, V. N., Nielsen, L. & Fink, A. L. Is Congo red an amyloid-specific dye? *J. Biol. Chem.* **276,** 22715–22721 (2001).
7. Bely, M. & Makovitzky, J. Sensitivity and specificity of Congo red staining according to Romhanyi. Comparison with Puchtler's or Bennhold's methods. *Acta Histochem.* **108,** 175–180 (2006).
8. Schütz, A. K. *et al.* The Amyloid-Congo Red Interface at Atomic Resolution. *Angew. Chem. Int. Ed. Engl.* **50,** 5956–5960 (2011).
9. Miura, T., Yamamiya, C., Sasaki, M., Suzuki, K. & Takeuchi, H. Binding mode of Congo Red to Alzheimer's amyloid beta-peptide studied by UV Raman spectroscopy. *J. Raman Spectrosc.* **33,** 530–535 (2002).
10. Ojala, W. H., Ojala, C. R. & Gleason, W. B. The X-Ray Crystal-Structure of the Sulfonated Azo-Dye Congo-Red, a Nonpeptidic Inhibitor of Hiv-1 Protease Which Also Binds to Reverse-Transcriptase and Amyloid Proteins. *Antiviral Chem. Chemother.* **6,** 25–33 (1995).
11. Kentgens, A., De Boer, E. & Veeman, W. S. Ultraslow Molecular Motions in Crystalline Polyoxymethylene - a Complete Elucidation Using Two-Dimensional Solid-State NMR. *J. Chem. Phys.* **87,** 6859–6866 (1987).
12. Hagemeyer, A., Schmidt-Rohr, K. & Spiess, H. W. Two-Dimensional Nuclear Magnetic Resonance Experiments for Studying Molecular Order and Dynamics in Static and in Rotating Solids. *Adv. Magn. Opt. Reson.* **13,** 85–130 (1989).
13. Tycko, R. & Berger, A. E. Dual processing of two-dimensional exchange data in magic angle spinning NMR of solids. *J. Magn. Reson.* **141,** 141–147 (1999).
14. Weliky, D. P. & Tycko, R. Determination of peptide conformations by two-dimensional magic angle spinning NMR exchange spectroscopy with rotor synchronization. *J. Am. Chem. Soc.* **118,** 8487–8488 (1996).
15. Smith, A. A. *et al.* Partially-deuterated samples of HET-s(218-289) fibrils: assignment and deuterium isotope effect. *J Biomol Nmr* **67,** 109–119 (2017).
16. van Beek, J. D. matNMR: a flexible toolbox for processing, analyzing and visualizing magnetic resonance data in Matlab. *J. Magn. Reson. Ser. A* **187,** 19–26 (2007).
17. Herzfeld, J. & Berger, A. E. Sideband Intensities in NMR-Spectra of Samples Spinning at the Magic Angle. *J. Chem. Phys.* **73,** 6021–6030 (1980).
18. Eichele, K. HBA: Herzfeld-Berger analysis program. *http://anorganik.uni-tuebingen.de/klaus/soft/index.php?p=hba/hba* **Version 1.7.5,** (2015).
19. Smith, S. A., Levante, T. O., Meier, B. H. & Ernst, R. R. Computer-Simulations in Magnetic-Resonance - an Object-Oriented Programming Approach. *J. Magn. Reson. Ser. A* **106,** 75–105 (1994).
20. Van Dongen Torman, J. & Veeman, W. S. C-13 Chemical Shielding Tensors in Para-Xylene. *J. Chem. Phys.* **68,** 3233–3235 (1978).
21. Raleigh, D. P., Levitt, M. H. & Griffin, R. G. Rotational Resonance in Solid-State Nmr. *Chem. Phys. Lett.* **146,** 71–76 (1988).
22. Bak, M., Rasmussen, J. T. & Nielsen, N. C. SIMPSON: A general simulation program for solid-state NMR spectroscopy. *J. Magn. Reson.* **147,** 296–330 (2000).
23. Tycko, R., Weliky, D. P. & Berger, A. E. Investigation of molecular structure in solids by two-dimensional NMR exchange spectroscopy with magic angle spinning. *J. Chem. Phys.* **105,** 7915–7930 (1996).
24. Facelli, J. C., Grant, D. M. & Michl, J. C-13 Shielding Tensors - Experimental and Theoretical Determination. *Acc. Chem. Res.* **20,** 152–158 (1987).